Sub-nT resolution of Single Layer Sensor Based on the AMR Effect in $La_{2/3}Sr_{1/3}MnO_3$ Thin Films

Luiz Guilherme Enger[1], Stéphane Flament[1], Imtiaz-Noor Bhatti[1], Bruno Guillet[1], Marc Lam Chok Sing[1], Victor Pierron[1], Sylvain Lebargy[1], Jose Manuel Diez[2], Arturo Vera[2], Isidoro Martinez[2], Ruben Guerrero[2], Lucas Perez[2,3], Paolo Perna[2], Julio Camarero[2], Rodolfo Miranda[2], Maria Teresa Gonzalez[2] and Laurence Méchin[1]

[1]Normandie Univ, UNICAEN, ENSICAEN, CNRS, GREYC, 14000 Caen, France

[2]IMDEA Nanociencia, Campus de Cantoblanco, 28049 Madrid, Spain

[3]Dept. Fisica de Materiales - Universidad Complutense de Madrid, Av. Complutense s/n 28040 Madrid, Spain

Single layer magnetoresistive sensors were designed in a Wheatstone bridge configuration using $La_{2/3}Sr_{1/3}MnO_3$ ferromagnetic oxide thin film. Uniaxial anisotropy was induced by performing epitaxial deposition of the films on top of vicinal $SrTiO_3$ substrate. X-ray scan confirms high crystalline quality of the films and the magnetic anisotropy was checked by Magneto-optical Kerr Effect measurements. Thanks to the anisotropic magnetoresistive effect and the very low noise measured in the devices, sub-nT resolution was achieved above 100 Hz at 310 K.

***Index Terms*—magnetic sensor, anisotropic magnetoresistance, uniaxial anisotropy, planar Hall effect bridge sensor, functional oxide, $La_{2/3}Sr_{1/3}MnO_3$ thin film**

I. Introduction

DUE to low cost, small size and increased performance of magnetoresistive sensors, they can be used in a wide range of applications such as biomedical, flexible electronics, position sensing, human-computer interaction, non-destructive evaluation and monitoring, navigation and transportation [1]. While giant magnetoresistance (GMR) [2] and tunneling magnetoresistance (TMR) [3] devices present electrical resistance variations due to the relative magnetization directions between two separate layers of ferromagnetic material, anisotropic magnetoresistance (AMR) devices have a resistance variation as function of the angle between magnetization and current density directions in the same layer. GMR and TMR thus required the stacking of different material layers, with a high precision on thickness and composition. Variations at buffer layer level provoke changes in sensor performance [4]–[7]. In the present work we fabricated AMR sensors made of a single layer of semi-metallic $La_{2/3}Sr_{1/3}MnO_3$ (LSMO) thin film, an oxide that is ferromagnetic up to 350 K [8] and presents a very low instrinsic noise in low frequencies [9]. Thin films were etched in Wheatstone bridge configuration, forming a device known in literature as Planar Hall Effect Bridge (PHEB) [10]–[12]. Usual PHEB sensors based on permalloy use either exchange bias or shape anisotropy to induce a magnetic easy axis. In this paper, such axis is obtained by step-induced magnetic uniaxial anisotropy [13]. To study the viability for biomedical applications of our sensors, samples were kept at 310 K temperature for magnetotransport and noise characterization. A dedicated low noise amplifier was used to qualify the resolution of the sensors which is in the sub-nT range".

Manuscript received March 16, 2021; revised xx, 2021. Corresponding author: S. Flament (email: stephane.flament@ensicaen.fr).

II. Film and Samples Characteristics

A Pulsed Laser Deposition system from TSST company was used to grow epitaxial LSMO thin films on top of vicinal $SrTiO_3$ (STO) substrate. After thin film deposition, LSMO was covered with gold for electrical contact, followed by standard UV lithography. Gold pads for electrical contact were defined with KI wet etching, and LSMO structure was obtained with Ion Beam Etching. Two Wheatstone bridge geometries were etched over each sample, as shown in Fig. 1. Wheatstone bridges with arms either parallel or perpendicular to sample easy axis are named 90WB sensor while Wheatstone bridges with arms at 45° to easy axis are named 45WB. In both geometries, each arm is 300 μm long and 100 μm large.

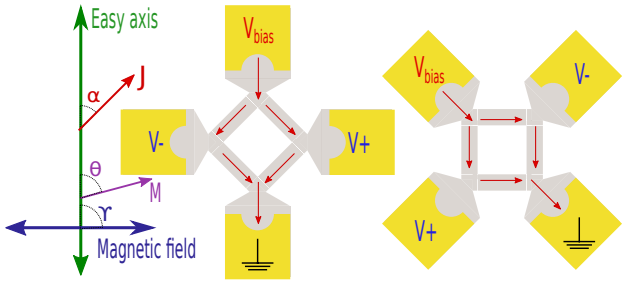

Fig. 1: Easy axis, current density J, magnetization M, applied magnetic field directions and PHEBs designs. 45WB (left) and 90WB (right) geometries.

The vicinal substrates present a surface miscut angle regarding the crystallographic plane, forming steps in the crystalline structure. This results in an easy magnetic axis parallel to step edges and enhances AMR effect [14]. In this paper we focus on results obtained with 4° vicinal angle STO substrate and LSMO film thicknesses of 30 nm and 60 nm. The rate of film growth was calibrated following the Reflective High-

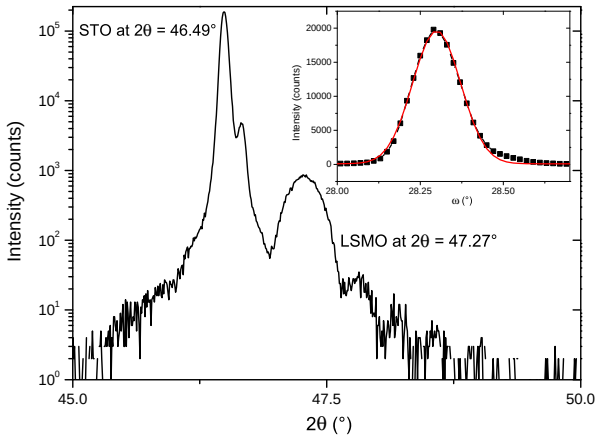

Fig. 2: 2θ XRD scan of 30 nm LSMO on 4° vicinal STO. Inset is LSMO rocking curve with gaussian fit.

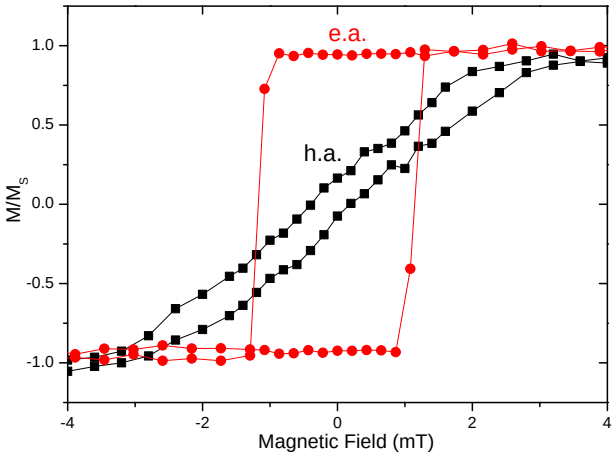

Fig. 3: Magnetization loops at room temperature of 60 nm thick LSMO thin film. Easy axis (e.a.) and hard axis (h.a.) along directions parallel and perpendicular to step edges, respectively.

Energy Electron Diffraction signal using a flat STO substrate. The exact thickness after deposition on vicinal STO was not measured. During film deposition, the laser power was kept at 1.7 J·cm^{-2}, the fire rate fixed at 3 Hz and the substrate temperature was kept at 730 °C. Structural analysis of LSMO over 4° vicinal STO was performed with θ-2θ X-ray diffraction (XRD) technique, as shown in Fig. 2. Peak signals for STO and LSMO were obtained at an offset ω angle of 4.74°. Deviation around the expected 4° angle are within accepted values due to substrate fabrication process and alignment in XRD sample holder. Rocking curve for LSMO with a Full Width at Half Maximum of 0.17° indicates high crystalline quality.

Uniaxial magnetic anisotropy in the etched PHEBs was verified with magnetization loops obtained using a lab-made longitudinal Magneto Optical Kerr Effect (MOKE) imaging setup. Local magnetization was deduced by averaging the MOKE intensity over the arms of the Wheatstone bridge [15]. As exhibited in Fig. 3, a hysteretic behavior typical of easy axis occurs when magnetic field is parallel to step edges while a linear dependence is observed when sample is rotated by 90°, indicating a hard axis magnetization along a direction perpendicular to step edges.

III. AMR Curves and Detectivity of Sensors

For MR and noise characterization, samples were loaded into a chamber with independent temperature and magnetic field control and equipped with four probes for electrical contact. MR curves were obtained with an amplitude sweep for magnetic field applied along hard axis, from one saturation state to the other and back. Noise measurements were carried out in environmental magnetic field, we did not make use of any magnetic shielded room. Taking advantage of the fact that a balanced Wheatstone bridge reject common-mode signals and noise, a commercial DC voltage source could be used to bias the samples. For signal amplification, we built a low-noise amplifier based on commercially available AD8421. Noise characteristics of this amplifier ensure that it is lower than the noise source of the Wheatstone bridge sensor, with a measured 3.6 nV·Hz$^{-1/2}$ broadband voltage noise and a negligible current noise in the resistance range of our samples: 6.1 kΩ resistance for 30 nm thick Wheatstone bridge and 2.5 kΩ for 60 nm sample. Figure 4 presents the measured noise of the 60 nm thick sample compared to the amplifier voltage noise, obtained at grounded inputs. Curve at 0 V bias includes the contribution from the amplifier voltage and current noises and from the sample thermal noise. As can be seen in the noise curve at 20 V bias, contribution from sample itself dominates the total noise. Both MR and noise were measured for different

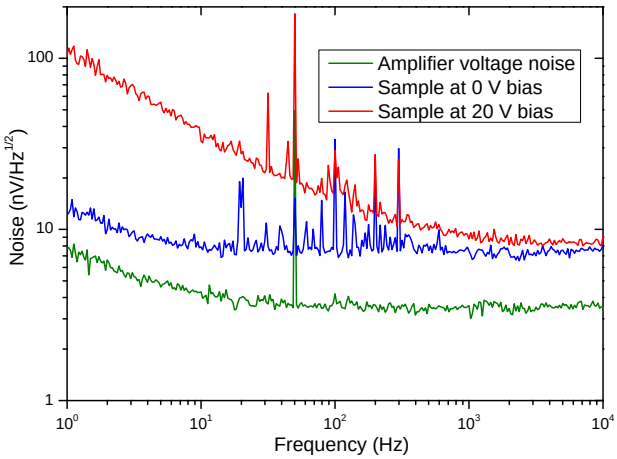

Fig. 4: Noise from 60 nm 45WB sample at 310 K and amplifier at room temperature.

voltage bias. Magnetoresistance curves for each geometry and for both samples are presented in Fig. 5. Both geometries present the expected MR curve for PHEB sensors. 45WB presents a linear response and a best sensitivity around zero applied field [10] while 90WB requires a DC magnetic bias to operate in a linear mode and at best sensitivity [16], around half of the maximum of the voltage output. The sensitivity S is deduced from MR measurements in the linear operating mode of the sensors by

$$S = \frac{\partial V_{out}}{\partial \mu_0 H} \quad (1)$$

It increases with higher MR ratio and lower anisotropy field [11]. The detectivity at a given bias, which is expressed in T·Hz$^{-1/2}$, is given by

$$D = \frac{\text{Noise}}{\text{Sensitivity}} \tag{2}$$

and calculated using experimental noise and sensitivity data. Better sensor performance means lower detectivity, therefore lower noise, higher MR ratio and lower anisotropy field. We observed that the thicker sample presents a higher MR ratio, while 30 nm sample has lower anisotropy field. It was reported that film thickness does affect step-induced magnetic anisotropy [13] but a complete theory for the magnetotransport in LSMO thin films at low field is not fully developed. Obtained sensitivity values are 58 %·T^{-1} (122 %·T^{-1}) for 45WB (90WB) structure in 60 nm sample, and 82 %·T^{-1} (125 %·T^{-1}) for 45WB (90WB) design with 30 nm LSMO. While the value of V_{meas} derivative was obtained at zero applied field for 45WB structure, in 90WB bridges an absolute value for bias field of 0.4 mT and 0.2 mT was considered for 60 nm and 30 nm samples, respectively. Ultimately, the thinner sample presents higher sensitivity value and thicker sample yielded a lower noise overall since its resistance is lower. Following (2), we plotted detectivity curves for both samples and both geometries, as shown in Fig. 6. Due to lower MR ratio presented in 45WB geometry, we had to increase the voltage bias of the bridge. In the four cases, we are able to reach sub-nT detectivities above 100 Hz. Even though 30 nm thick sample has higher sensitivity, a better performance is achieved with 60 nm thick sample thanks to lower intrinsic noise.

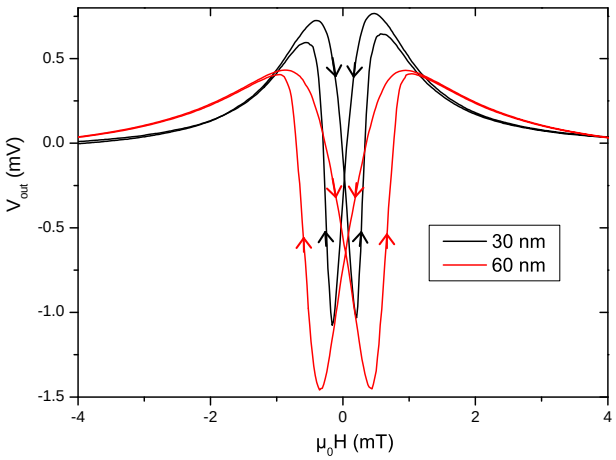

(a)

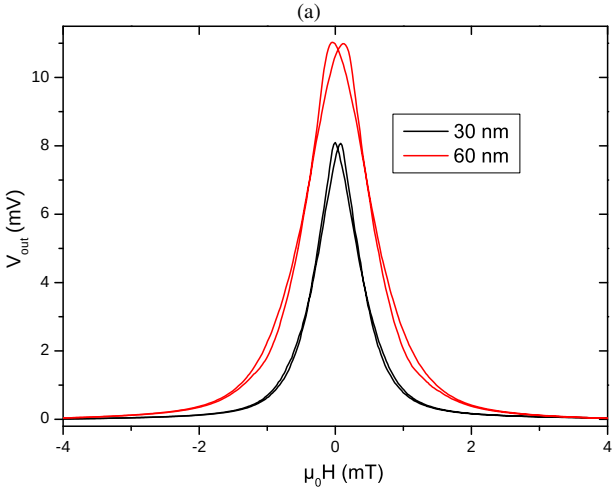

(b)

Fig. 5: AMR curves at 310 K sample temperature and 10 V bridge bias. (a) 45WB bridge design. (b) 90WB design.

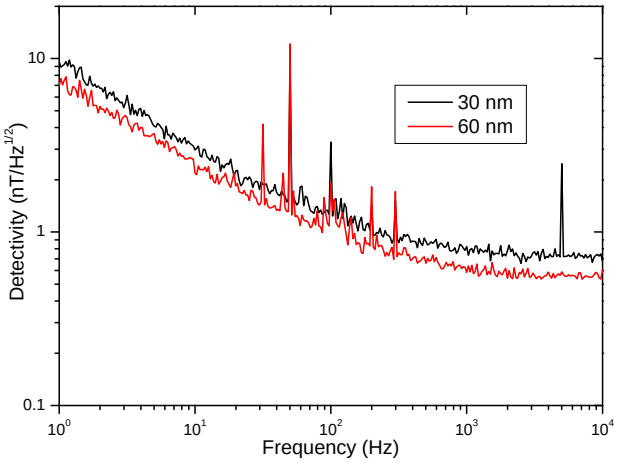

(a)

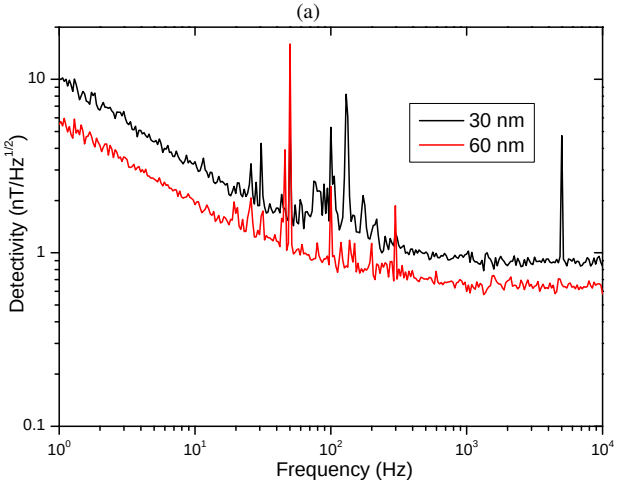

(b)

Fig. 6: (a) Detectivity of 45WB PHEB design at 20 V bias. (b) Detectivity of 90WB PHEB design at 10 V bias.

In the low frequency noise domain, a squared dependence of low-frequency noise on bridge voltage bias was obtained. This indicates that our sensor dominates the noise signal and presents a 1/f noise that can be modeled after Hooge's empirical equation [17] :

$$S_V = \frac{\alpha_H}{n}\frac{1}{f\Omega}V_{bias}^2 \tag{3}$$

where S_V is the spectral noise density expressed in V^2·Hz^{-1}, Ω is the volume of the Wheatstone bridge and n is the charge carrier density. In Fig. 7 we plot $S_V \times f$ for different voltage bias. A linear fit with a fixed slope of 2 shows that the squared dependence is verified. The S_V/V^2 versus f slope can be used as a comparison parameter between sensors. The lower this value, the better. For the 60 nm thick sample, it is

calculated equal to $4.3{\cdot}10^{-17}$. This value is a few orders of magnitude smaller that the one obtained in magnetic tunnel junctions and TMR sensors [18], [19], which explains why the Wheatstone bridge sensors presented in this paper achieve a good detectivity in the low frequency region albeit much lower sensitivity values than TMR sensors.

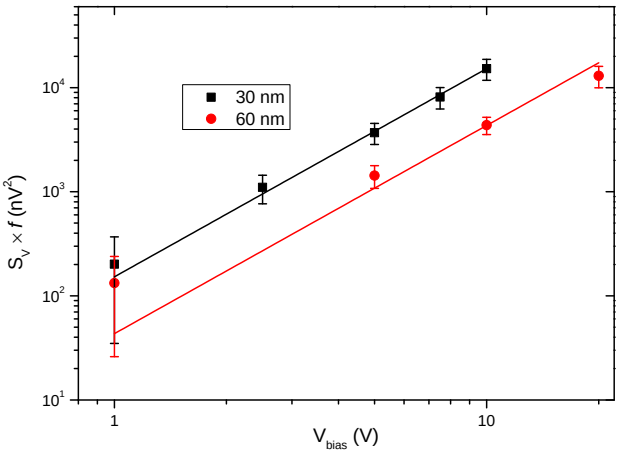

Fig. 7: Each $S_V \times f$ point is the average value from 1 to 10 Hz, error bars correspond to two standard deviations.

IV. Conclusion

By employing vicinal STO substrates and performing epitaxial LSMO deposition, we fabricated single layer AMR sensors without relying on exchange bias interaction or shape anisotropy. This is the first report on the realization of an actual Wheatstone bridge sensor based on manganite oxide and with a sub-nT resolution. θ-2θ XRD scan and LSMO rocking curve shows a high crystalline quality for the ferromagnetic oxide and a epitaxial growth along the slightly tilted axis of the vicinal substrates. Magnetization curves obtained on etched sample confirms uniaxial magnetic anisotropy, and outputs of the two presented PHEBs geometries are as expected, with the 45WB geometry being linear around zero field and the 90WB geometry needing a DC bias magnetic field. Noise measurements were carried out with a dedicated lab-made low-noise amplifier. Experimental data show that sub-nanotesla detectivity values is reached above 100 Hz at 310 K for both geometries. Despite its slighty poorer detectivity, the 45WB is preferable since it operates at zero field with a linear range adapted to its detectivity. The performance of the sensors may be improved with the addition of flux concentrators [20], by the use of modulation techniques [21] and with further studies on how tuning fabrication for a better detectivity.

Acknowledgment

This project has received funding from the European Union Horizon 2020 research and innovation program under grant agreement No 737116.

References

[1] C. Zheng, K. Zhu, S. Cardoso de Freitas, J. Chang, J. E. Davies, P. Eames, P. P. Freitas, O. Kazakova, C. Kim, C. Leung, S. Liou, A. Ognev, S. N. Piramanayagam, P. Ripka, A. Samardak, K. Shin, S. Tong, M. Tung, S. X. Wang, S. Xue, X. Yin, and P. W. T. Pong, "Magnetoresistive Sensor Development Roadmap (Non-Recording Applications)," *IEEE Trans. Magn.*, vol. 55, no. 4, 1–30, 2019. DOI: 10.1109/TMAG.2019.2896036.

[2] M. N. Baibich, J. M. Broto, A. Fert, F. N. Van Dau, F. Petroff, P. Etienne, G. Creuzet, A. Friederich, and J. Chazelas, "Giant magnetoresistance of (001)fe/(001)cr magnetic superlattices," *Phys. Rev. Lett.*, vol. 61, 2472–2475, 21 Nov. 1988. DOI: 10.1103/PhysRevLett.61.2472.

[3] M. Julliere, "Tunneling between ferromagnetic films," *Phys. Lett. A*, vol. 54, no. 3, 225–226, 1975, ISSN: 0375-9601. DOI: https://doi.org/10.1016/0375-9601(75)90174-7.

[4] G. Li, H. Shen, Q. Shen, T. Li, and S. Zou, "Influence of Si buffer layer on the giant magnetoresistance effect in Co/Cu/Co sandwiches," *Sci. China Ser. E-Technol. Sci.*, vol. 43, no. 4, 225–231, 2000. DOI: 10.1007/BF02916826.

[5] T. Li, H.-L. Shen, Q.-W. Shen, S.-C. Zou, K. Tsukamoto, and M. Okutomi, "Effects of Ni buffer layer on giant magnetoresistance in Co/Cu/Co sandwich," *J. Magn. Magn. Mater*, vol. 224, no. 1, 55–60, 2001, ISSN: 0304-8853. DOI: https://doi.org/10.1016/S0304-8853(00)01356-1.

[6] M. Sun, T. Kubota, S. Takahashi, Y. Kawato, Y. Sonobe, and K. Takanashi, "Buffer layer dependence of magnetoresistance effects in Co2Fe0.4Mn0.6Si/MgO/Co50Fe50 tunnel junctions," *AIP Adv.*, vol. 8, 055902, 2018. DOI: 10.1063/1.5007766.

[7] M. Sun, T. Kubota, Y. Kawato, S. Takahashi, A. Tsukamoto, Y. Sonobe, and K. Takanashi, "Buffer-Layer Dependence of Interface Magnetic Anisotropy in Co2Fe0.4Mn0.6Si Heusler Alloy Ultrathin Films," *IEEE Trans. Magn.*, vol. 53, no. 11, 1–4, 2017. DOI: 10.1109/TMAG.2017.2728627.

[8] J. Hemberger, A. Krimmel, T. Kurz, H.-A. Krug von Nidda, V. Y. Ivanov, A. A. Mukhin, A. M. Balbashov, and A. Loidl, "Structural, magnetic, and electrical properties of single-crystalline $La_{1-x}Sr_xMnO_3$ $(0.4 < x < 0.85)$," *Phys. Rev. B*, vol. 66, 094410, 9 Sep. 2002. DOI: 10.1103/PhysRevB.66.094410.

[9] L. Méchin, S. Wu, B. Guillet, P. Perna, C. Fur, S. Lebargy, C. Adamo, D. G. Schlom, and J. M. Routoure, "Experimental evidence of correlation between 1/f noise level and metal-to-insulator transition temperature in epitaxial $La_{0.7}Sr_{0.3}MnO_3$ thin films," *J. Phys. D Appl. Phys.*, vol. 46, no. 20, 202001, May 2013. DOI: 10.1088/0022-3727/46/20/202001.

[10] A. D. Henriksen, B. T. Dalslet, D. H. Skieller, K. H. Lee, F. Okkels, and M. F. Hansen, "Planar Hall effect bridge magnetic field sensors," *Appl. Phys. Lett.*, vol. 97, no. 1, 013507, 2010. DOI: 10.1063/1.3460290.

[11] A. D. Henriksen, G. Rizzi, and M. F. Hansen, "Experimental comparison of ring and diamond shaped planar Hall effect bridge magnetic field sensors," *J. Appl. Phys.*, vol. 118, 103901, 2015. DOI: 10.1063/1.4930068.

[12] A. Grosz, V. Mor, E. Paperno, S. Amrusi, I. Faivinov, M. Schultz, and L. Klein, "Planar hall effect sensors with subnanotesla resolution," *IEEE Magn. Lett.*, vol. 4, 6500104, 2013. DOI: 10.1109/LMAG.2013.2276551.

[13] D. S. Chuang, C. A. Ballentine, and R. C. O'Handley, "Surface and step magnetic anisotropy," *Phys. Rev. B*, vol. 49, 15084–15095, 21 1994. DOI: 10.1103/PhysRevB.49.15084. [Online]. Available: https://link.aps.org/doi/10.1103/PhysRevB.49.15084.

[14] P. Perna, D. Maccariello, F. Ajejas, R. Guerrero, L. Méchin, S. Flament, J. Santamaria, R. Miranda, and J. Camarero, "Engineering Large Anisotropic Magnetoresistance in $La_{0.7}Sr_{0.3}MnO_3$ Films at Room Temperature," *Adv. Funct. Mater.*, vol. 27, no. 26, 1700664, 2017. DOI: 10.1002/adfm.201700664.

[15] M. Saïb, M. Belmeguenai, L. Méchin, D. Bloyet, and S. Flament, "Magnetization reversal in patterned $La_{0.67}Sr_{0.33}MnO_3$ thin films by magneto-optical Kerr imaging," *J. Appl. Phys.*, vol. 103, no. 11, 113905, 2008. DOI: 10.1063/1.2938068.

[16] L. Quynh, B. Tu, D. Dang, D. Viet, L. Hien, D. Huong Giang, and N. Duc, "Detection of magnetic nanoparticles using simple AMR sensors in Wheatstone bridge," *J SCI-ADV MATER DEV*, vol. 1, no. 1, 98–102, 2016, ISSN: 2468-2179. DOI: https://doi.org/10.1016/j.jsamd.2016.04.006.

[17] F. Hooge, "1/f noise is no surface effect," *Phys. Lett. A*, vol. 29, no. 3, 139–140, 1969, ISSN: 0375-9601. DOI: https://doi.org/10.1016/0375-9601(69)90076-0.

[18] J. Y. Chen, J. F. Feng, and C. J. M. D., "Tunable linear magnetoresistance in mgo magnetic tunnel junction sensors using two pinned cofeb electrodes," *Appl. Phys. Lett.*, vol. 100, 142407, 2012. DOI: 10.1063/1.4978465. [Online]. Available: https://doi.org/10.1063/1.4978465.

[19] J. G. Deak, Z. Zhou, and W. Shen, "Tunneling magnetoresistance sensor with pt level 1/f magnetic noise," *AIP Advances*, vol. 7, 056676, 2017. DOI: 10.1063/1.3701277. [Online]. Available: http://dx.doi.org/10.1063/1.3701277.

[20] X. Zhang, Y. Bi, G. Chen, J. Liu, J. Li, K. Feng, C. Lv, and W. Wang, "Influence of size parameters and magnetic field intensity upon the amplification characteristics of magnetic flux concentrators," *AIP Advances*, vol. 8, no. 12, 125222, 2018. DOI: 10.1063/1.5066271. [Online]. Available: https://doi.org/10.1063/1.5066271.

[21] L. Caruso, T. Wunderle, C. M. Lewis, J. Valadeiro, V. Trauchessec, J. T. Rosillo, J. P. Amaral, J. Ni, P. Jendritza, C. Fermon, S. Cardoso, P. P. Freitas, P. Fries, and M. Pannetier-Lecoeur, "In vivo magnetic recording of neuronal activity," *Neuron*, vol. 95, 1283–1291.e4, 2017. DOI: 10.1016/j.neuron.2017.08.012. [Online]. Available: http://dx.doi.org/10.1016/j.neuron.2017.08.012.

Luiz Guilherme Enger was born in Lajeado, Brazil, in 1994. He received a five-year engineering degree in Engineering Physics from the Federal University of Rio Grande do Sul, Porto Alegre, Brazil, in 2017. He is currently pursuing the Ph.D degree in Microelectronics at Université de Caen Normandie, Caen, France. His current research interests include magnetic field sensors, biomedical and industrial applications, modeling and numerical simulations.

Stéphane Flament received the PhD Degree in electrical engineering from the University of Caen, France, in 1994. He is currently Professor, member of the GREYC - CNRS lab, Caen, France. He worked on effects of Abrikosov vortices in superconductive devices and sensors, imaging of vortices using the magneto-optical Faraday effect and local magnetization distribution using the Kerr effect. His current research deals with the development of magnetoresistive sensors based on functional oxides.

Imtiaz-Noor Bhatti obtained a Ph'D in physics from Jawaharlal Nehru University, New Delhi, India, in 2019. His main research topic is experimental condensed matter physics. He also works in designing and developing new techniques for characterizing materials.

Bruno Guillet received the PhD and the accreditation to supervise research in Electronics-Microelectronics from the University of Caen, France, respectively in 2003 and in 2014. He is currently an associate professor in electronics with the University of Caen. His research interests include design, fabrication, and characterization of innovative materials such as functional oxides and nitrides for sensors and components. In GREYC laboratory, he is working on noise measurements, resistive thermometry and bolometers. He has authored or co-authored 48 publications in peer-review journals.

Marc Lam Chok Sing holds an Electrical Engineering degree from Caen National School of Engineering and received the Ph.D. degree in science from the University of Caen, France. He is currently a Lecturer in electronics and carries out his research within the GREYC CNRS laboratory at Caen, France. His present research interests include functional oxides magnetoresistive sensors, and low-noise electronics.

Victor Pierron received the Master Degree in Surface Engineering from the University of Strasbourg, France, in 2017. He is currently a CNRS engineer in elaboration of thin-film materials with GREYC, Caen, France. He is the technical support in the clean room manufacturing process.

Sylvain Lebargy received the superior degree for Technician in Grainville, France, in 1992. He is currently a research engineer at GREYC, University of Caen, Caen, focused in analog and digital circuits for sensing devices and low noise. He is the technical support in circuits conception and analysis.

Jose Manuel Diez

Arturo Vera

Isidoro Martinez

Ruben Guerrero

Lucas Perez

Paolo Perna obtained the BCs + MCs in Theoretical Physics on 2003 at the University Federico II in Naples (Italy) and then moved to the experimental research. On 2008, he obtained two PhD titles in Physics: Condensed Matter and Devices from the University of Caen Basse-Normandie (France) and in Mechanical Engineering (Material Science) from the University of Cassino (Italy). He is Research. Prof. at IMDEA Nanoscience leading the SpinOrbitronics group. His research activities cover both fabrication and characterization of magnetic and non-magnetic systems focusing on their fundamental properties and potential technological applications

Julio Camarero received his Ph.D in physics from the Universidad Autónoma de Madrid (UAM) in 1999. He then worked at Institut Neel-CNRS France (Marie- Curie Fellow and scientific contracts) before returning to UAM in 2003 as Ramon y Cajal research fellow. He is currently Associate Professor of the Condensed Matter Physics Department. In 2008 he joined IMDEA Nanoscience as Associated Senior Scientist, leading the Nanomagnetism Program. He has coordinated National Regional and European projects and has published more than 80 peer-reviewed papers, 11 book chapters, 4 invited papers, and 1 EU patent.

Rodolfo Miranda got his Ph.D in Physics from the Universidad Autónoma de Madrid (UAM) in 1981 for a work on the role of defects on surfaces. He worked in Munich and Berlin with Gerhard Ertl (NL in Chemistry 2007), before being appointed Full Professor of Condensed Matter Physics at the UAM in 1990. Prof. Miranda has been Vice-chancellor of Research and Scientific Policy (1998-2002) of the UAM, Executive Secretary of the R+D Commission of the Conference of Rectors of Spanish Universities (CRUE) (2000-2002) and Director of the Materials Science Institute "Nicolas Cabrera". He has served on Advisory Committees for different institutions, such as the Surface Science Division of IUVSTA, the Max Planck Institute fur Mikrostruktur Physik or the European Synchrotron Radiation Facility (ESRF). Prof. Miranda is Fellow of the American Physical Society since 2007, Head of the Surface Science Lab of the UAM (LASUAM) and Director of the Madrid Institute for Advanced Studies in Nanoscience (IMDEA-Nanociencia) from February 2007. Prof. Miranda's research interests range from low dimensional magnetism or molecular self-organization on surfaces to the mechanisms of epitaxial growth, the growth and properties of graphene or the use of magnetic nanoparticles in nanomedicine.

Teresa Gonzalez got her PhD in Physics (2003) at the Universidad de Santiago de Compostela in Spain, awarded as Outstanding Doctorate. She is an expert in electrical transport properties of matter. She has worked in different fields including superconductivity, molecular electronics, and more recently, the recording and stimulation of electric impulses at the nervous tissue. She worked as a postdoctoral researched at the Universität Basel in Christian Schönenberger's group (2004-2008), and then joined the Fundación IMDEA Nanociencia in Madrid in 2008, where continues to work. She is presently head of the IMDEA Neural Interfaces Laboratory.

Laurence Méchin received the PhD Degree in electrical engineering from the University of Caen, France, in 1996. She is currently a CNRS Senior Scientist with GREYC, Caen, France. She has authored or co-authored more than 120 papers. Her research interests are the design, fabrication, and characterization of innovative materials such as functional oxides and nitrides for sensors and components.